Examination of HER3 targeting in cancer using monoclonal antibodies

Nadège Gaborit[a], Ali Abdul-Hai[a,b], Maicol Mancini[a], Moshit Lindzen[a], Sara Lavi[a], Orith Leitner[c], Lucile Mounier[d], Myriam Chentouf[e], Sai Dunoyer[a], Manjusha Ghosh[a], Christel Larbouret[e], Thierry Chardès[e], Hervé Bazin[d], André Pèlegrin[e], Michael Sela[f,1], and Yosef Yarden[a,1]

Departments of [a]Biological Regulation, [f]Immunology, and [c]Biological Services, Weizmann Institute of Science, Rehovot 76100, Israel, [e]Institut de Recherche en Cancérologie de Montpellier, INSERM, U896, Montpellier, France; [d]Cisbio Bioassays, Innovation Management, Parc Marcel Boiteux, 30200 Codolet, France; and [b]Department of Internal Medicine, Kaplan Medical Center, Rehovot 76100, Israel

Contributed by Michael Sela, December 11, 2014 (sent for review August 4, 2014)

The human EGF receptor (HER/EGFR) family of receptor tyrosine kinases serves as a key target for cancer therapy. Specifically, EGFR and HER2 have been repeatedly targeted because of their genetic aberrations in tumors. The therapeutic potential of targeting HER3 has long been underestimated, due to relatively low expression in tumors and impaired kinase activity. Nevertheless, in addition to serving as a dimerization partner of EGFR and HER2, HER3 acts as a key player in tumor cells' ability to acquire resistance to cancer drugs. In this study, we generated several monoclonal antibodies to HER3. Comparisons of their ability to degrade HER3, decrease downstream signaling, and inhibit growth of cultured cells, as well as recruit immune effector cells, selected an antibody that later emerged as the most potent inhibitor of pancreatic cancer cells grown as tumors in animals. Our data predict that anti-HER3 antibodies able to intercept autocrine and stroma–tumor interactions might strongly inhibit tumor growth, in analogy to the mechanism of action of anti-EGFR antibodies routinely used now to treat colorectal cancer patients.

antibody combination | cancer therapy | HER3 | signal transduction | tyrosine kinase

Growth factors and their plasma-membrane–embedded receptors regulate cellular proliferation and migration during both embryogenesis and oncogenesis (1). One example entails the epidermal growth factor (EGF) family and the corresponding human EGF receptor (HER)/ERBB family of four receptor tyrosine kinases: the EGF receptor (EGFR or ERBB1), HER2 (c-Neu or ERBB2), HER3 (ERBB3), and HER4 (ERBB4) (2). The intracellular parts of ERBB/HER receptors harbor a catalytic tyrosine kinase domain (3). After ligand binding to an ectodomain, these receptors form active homodimers or heterodimers (4–7). Unlike EGFR, HER3/ERBB3 presents very low tyrosine kinase activity (8). Nevertheless, it binds neuregulins (NRGs) and exerts profound influence on signaling pathways, primarily through dimerization with EGFR and HER2. In line with roles in cancer progression, and similarly to EGFR and HER2, mutant forms of HER3 have recently been reported in colon and gastric cancer (9).

Cancer therapies that use monoclonal antibodies (mAbs) to target ERBB/HER family members are becoming a mainstay in oncology. For example, trastuzumab, which targets HER2, is currently used to treat gastric and breast cancer (10, 11). However, the majority of patients with metastatic HER2-positive breast cancer will become trastuzumab-resistant after prolonged treatment, a development significantly less common in an adjuvant or neo-adjuvant setting. It has been reported that trastuzumab-resistant tumors show elevated expression of HER3 (12), and, similarly, inhibition of HER2 using a kinase inhibitor also upregulates HER3 (13). Likewise, HER3 has been implicated in the development of resistance to treatment with other ERBB/HER-targeted therapies (14, 15), agents blocking insulin-like growth factor receptors (16), and chemotherapeutic agents (17). For these reasons, anti-HER3 antibodies (Abs) are being developed by several laboratories, and some have reached initial clinical trials.

Importantly, anticancer mechanisms of therapeutic Abs are multifactorial and incompletely understood. The involvement of Ab-dependent cellular cytotoxicity (ADCC) and complement-dependent cytotoxicity, as well as various cellular processes such as triggering of apoptosis, blocking angiogenesis, inhibiting tumor cell proliferation, interfering with signaling cascades, and accelerating receptor internalization, have been described (18). Our own studies proposed critical involvement of the endocytic system. In particular, combinations of two mutually noncompetitive Abs (Abs against different epitopes that do not cause steric hindrance) to EGFR (19) or to HER2 (20, 21) have been shown to accelerate receptor endocytosis and inhibit tumor growth, better than either Ab alone. Furthermore, a recently completed clinical trial that combined with chemotherapy two mutually noncompetitive anti-HER2 mAbs, for the treatment of HER2-positive breast cancer (22), confirmed the clinical benefit of combining noncompetitive mAbs.

Anti-HER3 agents that are being developed or are in clinical trials show promising results, yet their efficacy might be viewed, in general, as variable and rather modest (23). Hence, it is imperative to develop new agents and resolve their molecular mechanisms of action. In this study, we generated in mice a relatively broad series of anti-HER3 mAbs and examined them for the ability to both degrade HER3 and decrease downstream signaling.

Significance

The human EGF receptor (EGFR/HER) family plays critical roles in tumor progression. Therefore, several therapies intercepting these receptors were developed and clinically approved. Importantly, patients treated with such therapeutics often develop resistance, and in some cases this resistance has been associated with activation of HER3. Potentially, HER3 blockade might overcome patient resistance. Hence, antibodies to HER3 have been developed by us and other researchers. However, it has remained unclear which antibody attributes are required for effective tumor inhibition. To address this issue, we generated several monoclonal antibodies, which were tested in vitro and in tumor-bearing animals. Our results suggest that anti-HER3 antibodies able to intercept stroma–tumor interactions, as well as accelerate HER3 degradation, might inhibit tumor growth better than other antibodies.

Author contributions: N.G., M.S., and Y.Y. designed research; N.G., A.A.-H., M.M., M.L., S.L., O.L., L.M., M.C., S.D., M.G., and H.B. performed research; C.L., T.C., and A.P. contributed new reagents/analytic tools; N.G., M.S., and Y.Y. analyzed data; and N.G. and Y.Y. wrote the paper.

The authors declare no conflict of interest.

[1]To whom correspondence may be addressed. Email: yosef.yarden@weizmann.ac.il or michael.sela@weizmann.ac.il.

This article contains supporting information online at www.pnas.org/lookup/suppl/doi:10.1073/pnas.1423645112/-/DCSupplemental.

The new mAbs displayed a variety of biochemical and biological attributes, such as binding affinity to HER3, ability to displace NRG and block downstream signals, sort HER3 for degradation, and recruit natural killer cells. Ultimately, the Abs were tested in vitro and in tumor-bearing animals for their ability to inhibit growth of cancer cells. We focus on an especially potent tumor-inhibitory Ab that can displace NRG, robustly sort HER3 for intracellular degradation, and also recruit immune effector cells.

Results

Generation of mAbs Against the Extracellular Domain of HER3. To extend our previously described set of Abs to HER3 (24), a fusion protein combining the extracellular domain of HER3 and the Fc domain of a human IgG1 (denoted IgB3; Fig. S1*A*) was produced and used for the immunization of mice. We screened hybridoma supernatants by ELISA on IgB3-coated microplates and also performed negative selection on human IgG-coated microplate (Fig. S1*B*). The positive hybridoma supernatants were checked for their capacity to bind with the native form of HER3 by using an immunoprecipitation assay (Fig. S1*C*), and the corresponding hybridomas were subcloned. Twelve positive hybridomas were selected. Partial nucleotide sequencing of cDNAs encoding the heavy and light chains identified four distinct groups of Abs. These Abs were isotyped and identified as IgG1 molecules with kappa chains (Fig. S1*D*). Our subsequent studies used six mAbs: four from the new generation (NG33, NG83, NG140, and NG533) and two from the previous generation (XC90 and XC252) (24). Interestingly, the data reported in Fig. S1*E* indicate that NG83 was able to recognize the denatured form of HER3 in Western blots.

The Generated Abs Recognize Specifically and with High Affinity the Native Form of HER3. A comparison of the capacity of purified mAbs to bind with a native IgB3 was performed by using ELISA (Fig. 1*A*). The EC_{50} of our mAb for IgB3 binding ranged between 0.21 nM (XC252) and 16.8 nM (NG140). Next, we compared mAb ability to bind to the native form of the receptor using FACS and NIH/3T3-R2R3 cells, which co-overexpress ectopic HER2 and HER3 (25) (Fig. 1 *B* and *C*). To define the affinity of each Ab to HER3, we used the Tag-lite technology (Fig. S2). Each Ab was labeled with the d2-dye. By using fluorescence resonance energy transfer and measuring binding of the labeled mAbs to cells presenting Lumi4(Tb)-labeled HER3, we determined individual K_D values and reported them in Table 1. The values we obtained correlated with the patterns of HER3 binding determined by FACS (Fig. 1 *B* and *C*), although they differed from the patterns of IgB3 binding (Fig. 1*A*). As expected, we were unable to determine the affinity of mAb NG533, because its ability to bind with the native form of HER3 was barely detectable using either FACS (Fig. 1 *B* and *C*) or immunoprecipitation (Fig. 1*D*). As expected by the nanomolar range of HER3 recognition by the new mAbs, we confirmed using FACS their specificity to HER3 and not to the other members of the HER/ERBB family (Fig. S3).

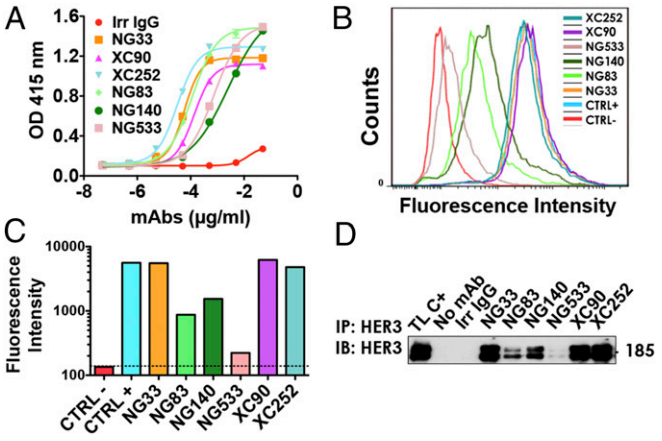

Fig. 1. A set of mAbs specifically targeting HER3. (*A*) The 96-well plates were coated by using a solution containing IgB3 (1.5 µg/mL) and thereafter incubated for 1 h with the indicated mAbs. After washing, a second 1-h-long incubation with HRP-labeled anti-mouse IgG was performed and followed by incubation for 20 min with 2,2′-azino-bis(3-ethylbenzothiazoline-6-sulfonic acid). Light absorbance (415 nm) signals are presented. (*B* and *C*) NIH/3T3-R2R3 cells were incubated for 60 min at 4 °C with the indicated mAbs (each at 10 µg/mL). After two washes, the cells were similarly incubated with a secondary anti-mouse IgG Ab coupled to Alexa Fluor 488. Fluorescence intensity (F.I.) signals were measured by using the LSRII flow cytometer. Positive and negative controls were used for reference. (*D*) Protein G beads were incubated first with the indicated mAbs (5 µg; for 2 h at 4 °C), and after two washes, the beads were incubated with cleared N87 cell lysate. After four washes, the immunoprecipitated (IP) proteins were separated by using electrophoresis and immunoblotting (IB) with an Ab to HER3/ERBB3.

Specific mAbs Trigger HER3 Degradation and Cell-Mediated Cytotoxicity. The mAbs' capacity to down-regulate HER3 was determined by using Western blotting. Gastric cancer N87 cells were treated for 3 h with each mAb (10 µg/mL), and HER3 expression levels were analyzed by using Western blotting (Fig. 2 *A* and *B*). NG33 induced more extensive degradation of HER3 compared with other mAbs. Next, we evaluated whether the effect observed in N87 cells was cell-type-dependent. Hence, we tested different cancer cell lines and observed similar patterns of receptor degradation (Fig. 2*C*). In addition, we compared the pattern of HER3 degradation using NG33 (10 µg/mL) to the signal obtained using NRG (20 ng/mL; Fig. S4). Interestingly, NG33 induced faster and more extensive receptor degradation than did NRG. Furthermore, the mAb ability to lead to ADCC was determined by using BXPC3-luc cells, which were incubated with the studied mAbs and with human mononuclear cells. Cell killing is reported in Fig. 2*D*. Note that we used trastuzumab as a positive control and observed medium to high signals with three mAbs: NG33, NG83, and NG533. In conclusion, the series of mAbs displayed variation in terms of Ab activities, and NG33 stood out as a relatively strong inducer of both ADCC and HER3 degradation.

Ab NG33 Competes with NRG for Binding to HER3. A competition assay between mAbs to HER3 and d2-labeled NRG molecules was used to identify mAbs able to reduce NRG binding to HER3 (Fig. 3*A*). NIH/3T3-R2R3 cells overexpressing an ectopic HER3 were treated with increasing concentrations of each mAb, under conditions that avoid HER3 internalization. Thereafter, the cells were incubated with the labeled NRG. The results indicated that NG33 was the only mAb able to effectively displace NRG. Notably, NG140 weakly competed with NRG, and both XC90 and XC252 slightly enhanced NRG binding. To check whether the effect on NRG binding has an impact on the phosphorylation of HER3 and downstream signaling, we treated N87 cells with each mAb for 20 min, followed by a short stimulation with NRG (Fig. 3*B*). Evidently, NG33 completely prevented NRG-induced HER3 phosphorylation and subsequent AKT and ERK activation. Similarly, XC252 was able to partly decrease the phosphorylation level of HER3, but this result might not be attributed to direct competition with NRG.

NG33 Inhibits NRG-Induced Migration and Proliferation of Cancer Cells. Next, we studied the impact of NG33, our NRG competitor mAb, on ligand-induced cell proliferation and migration. First, we evaluated the effect of NG33 on NRG-induced migration of ovarian cancer cells (Fig. 3*C*). The results confirmed that NG33 treatment reduced NRG-induced migration. Second, NG33's ability to influence survival of different cancer cells was

Table 1. K_d determinations using the Tag-Lite technology

mAbs	K_D, nM	SD, nM
NG33	2.96	0.66
NG83	>24	—
NG140	6.12	—
NG533	Un.	—
XC90	2.30	0.02
XC252	1.09	0.17

Cells were transfected with HER3–SNAP-Tag and labeled with BG-Lumi4(Tb), a SNAP-tag substrate. After incubation with increasing concentrations of the indicated d2-labeled mAb directed to HER3, the K_d was determined from binding curve fitting. The binding curve was obtained by measuring TR-FRET between the donor Lumi4(Tb) and the acceptor d2-dye. Un., undetermined.

evaluated in vitro by using the 3-(4,5-dimethylthiazol-2-yl)-2,5-diphenyltetrazolium bromide (MTT) assay (Fig. 4 *A* and *C*). Cells were first selected for their ability to proliferate following NRG stimulation. In several cancer cell lines (breast, MCF7 and SKBR-3; lung, NCI-H322M; ovarian, OVCAR-5; pancreatic, BXPC3; and gastric, N87), NG33 inhibited (20–50%) NRG-induced cell survival. Abs NG83, XC252, and XC90 were tested as well, but they exerted no marked inhibition. Similarly, NG83 did not impact survival, but this result might be explained by its relatively low binding affinity (Table 1). In conclusion, NG33 emerged from these studies as a potent inhibitor of cell growth, in line with effects on HER3 stability and blocking of NRG-induced signals.

NG33 Is as Effective as Trastuzumab in Inhibiting Growth of HER2-Overexpressing Cancer Cells both in Vitro and in Animals. To examine NG33's ability to decrease cancer cell growth, we focused on N87, a gastric cancer cell line overexpressing HER2 and co-expressing EGFR and HER3. The comparison of the geometric mean taken from the FACS experiment showed that N87 cells express 2.2-fold more HER2 than HER3 (Fig. 4*B*). Hence, we compared two different ways to decrease N87 cell growth: One approach used mAb NG33 to HER3, and the other used trastuzumab, a clinically approved therapeutic mAb directed against HER2. The effects of the Abs were compared both in vitro, by using a colorimetric assay on NRG-stimulated N87 cells, and in vivo, by using N87 cell xenografts (Fig. 4 *C* and *D*). The in vitro comparison was extended to additional cell lines (Fig. 4*A*). The results we obtained indicated that NG33 is as effective as trastuzumab in decreasing cancer cell growth in vitro and N87 tumorigenic growth in animals ($P < 0.05$).

Improvement of NG33's in Vitro Effects by Combinations with Other mAbs Directed to HER3. To try and improve the effects of NG33, our most potent mAb, we combined it with another anti-HER3 Ab. First, we determined which Ab of our anti-HER3 series could target an epitope distinct from that targeted by NG33. For this determination, we used a Lumi4(Tb)-labeled NG33 and IgB3-coated microplates (Fig. 5*A*). The results indicated that XC90 was the only mAb able to compete with NG33: NG140 and XC252 did not alter NG33 binding, and, interestingly, mAb NG83 potentiated NG33 binding to IgB3. These observations were corroborated by using a labeled form of XC252 (Fig. 5*B*). In the next step, we tested mAb combinations for their ability to degrade HER3 (Fig. 5*C*) and also decrease phosphorylation of HER3, AKT, and ERK (Fig. 5*D*). The HER3 degradation assays identified the mixtures NG33+NG83 and NG33+NG140 as suitable combinations. However, the analysis of NRG-induced phosphorylation of HER3, ERK, and particularly AKT favored the combinations NG33+XC252 and NG33+NG140.

The Combination of NG33 with a Second, Noncompetitive mAb Enhances the Inhibitory Effect on Cancer Cell Proliferation in Vitro and, to Some Extent, also in Animals. As a prelude to in vivo studies, we examined single mAbs, or their combinations with NG33, for their capacity to inhibit proliferation of BXPC3 pancreatic cells, which highly express NRG (26) (Fig. 6 *A*–*C*). Decreasing mAb concentrations were used, and a colorimetric assay was performed after 3 d of treatment. NG83 and NG140 used alone did not interfere with cell growth. However, at high concentrations, the combinations of NG33 and either NG83 or NG140 showed stronger inhibitory effects than NG33 alone (Fig. 6 *A* and *B*); conversely NG33 alone induced 38% inhibition of cell survival, and in combination with NG83 or NG140, the mAb induced 73% or 60% inhibition, respectively ($P < 0.0001$). By contrast, the combination of NG33 and XC252 showed no additive impact on cell growth (Fig. 6*C*), probably due to the relatively strong inhibition imposed by XC252 when singly applied.

To select an in vivo tumor model, a pilot animal experiment was conducted by using a mixture of our stronger in vitro inhibitors, NG33 and XC252, and a series of tumor cell lines (gastric, N87; lung, A549; pancreatic, BXPC3; ovarian, OVCAR-5; and head and neck, CAL-27; Fig. S5). This experiment was performed with only three mice per group. Mice were injected twice a week with the mAb combination or with saline. The best responder of these in vivo models was the pancreatic BXPC3 xenograft. Hence, the efficacy of three different mAb combinations was evaluated on the respective xenograft. This second animal study was performed on groups of seven or eight mice, which were treated once every 3 d with saline, single mAbs, or a mAb combination (total: 0.2 mg per injection). Tumor growth curves are reported in Fig. 6. The ability of NG33 to decrease tumor growth, compared with saline, was confirmed ($P < 0.0001$, after 3 wk of treatment). In this animal model, the other mAbs, NG83, NG140, and XC252, showed no statistically significant ability to decrease tumor growth when singly administered. However, the combination of NG83 (Fig. 6*D*) or NG140 (Fig. 6*E*) with NG33 showed a clear trend toward an improvement of NG33's antitumor efficacy. These trends did not reach statistical significance, but similar results were also obtained in a second experiment. Notably, in line with the in vitro study, the

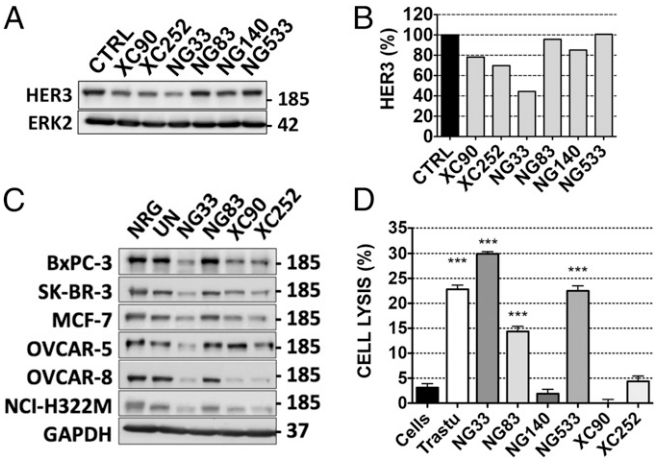

Fig. 2. Ab-dependent cell-mediated cytotoxicity and receptor degradation induced by anti-HER3 Abs. (*A* and *B*) N87 cells were treated for 3 h with the indicated mAbs. Protein samples were subjected to immunoblotting by using the indicated Abs, and signals were quantified. (*C*) The experiment shown in *A* was performed on six other cancer cell lines, except that GAPDH was used as a loading control. (*D*) Luciferase-expressing BXPC3 cells were incubated with the indicated mAbs and secondarily with human peripheral blood mononuclear cells (for 24 h). Cell killing was detected by measuring luminescence after the addition of luciferine. ***$P < 0.001$ (ANOVA and post hoc tests).

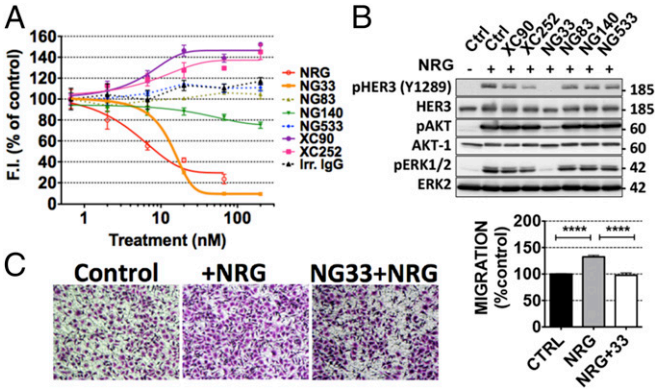

Fig. 3. The anti-HER3 mAb NG33 decreases NRG-induced phosphorylation of HER3, AKT, and ERK, as well as NRG-induced cell migration. (*A*) NIH/3T3-R2R3 cells coexpressing human HER2 and HER3 were plated on black microplates and incubated for 45 min at 4 °C with increasing concentrations of mAbs to HER3. After washing, we added a fluorescently labeled NRG and incubated for 30 min at 4 °C. Fluorescence intensities (at 670 nm) were determined after three washes. (*B*) The ability of the indicated mAbs to inhibit NRG-induced phosphorylation of HER3, AKT, and ERK was studied by using N87 cells, which were treated at 37 °C for 20 min with the indicated mAbs (10 μg/mL). NRG (20 ng/mL) was added to the cells and incubated for 10 min. The cells were then lysed, and equal quantities of protein lysates were resolved by using electrophoresis and immunoblotting, as indicated. (*C*) The capacity of mAb NG33 to inhibit NRG-induced migration was tested by using OVCAR-5 cells that were seeded in the upper compartment of migration chambers. The lower compartment of each chamber was filled with medium supplemented with NRG (10 ng/mL). After 24 h, cells that reached the lower side of the filter were fixed, permeabilized, and stained by using Giemsa. Signals of triplicates were quantified. ****$P < 0.0001$ (ANOVA and post hoc tests).

combination of NG33 with XC252 (Fig. 6*F*) was clearly as efficient as NG33 alone.

In summary, by generating a set of mAbs to HER3 and testing them in vitro for the ability to inhibit NRG binding, enhance HER3 degradation, retard downstream signaling, recruit immune effector cells, and arrest growth of cancer cells in vitro, we selected NG33 as the most promising candidate for animal studies. As expected, NG33 emerged from our animal tests as the best inhibitor of pancreatic tumor cells that secrete NRGs and express HER3. Our attempts to enhance NG33's anti-cancer effects by combining it with other, noncompetitive mAbs to HER3 yielded only limited added benefit. Hence, it is conceivable that NG33's therapeutic potential is due to an ability to inhibit NRG-mediated growth and migration of tumor cells in response to stromal cues.

Discussion

Because several lines of evidence have implicated HER3 in tumorigenesis (27–29), and because this binder of multiple NRG isoforms participates in the development of resistance to some cancer therapies (14–17), a few anti-HER3 mAbs have been generated (23, 27, 28, 30). Several studies, including those performed in our laboratory, previously described a strategy to enhance the antitumor activity of mAbs by combining two Abs directed to nonoverlapping epitopes of the shared antigen, for example, EGFR (19, 31) or HER2 (20, 21, 32, 33). When applied on cells, such mAb pairs showed enhanced ability to induce receptor endocytosis and inhibit tumor growth. We generated the first set of mAbs to HER3 soon after clarifying the relationships between the NRGs and their high (HER4) and low (HER3) affinity receptors (24). The herein-described new set of mAbs was aimed at understanding the relations between mAb identity and growth inhibition, as well as testing the relative potency of Ab combinations.

To study the effects of single mAbs on tumor growth, we selected BXPC3 human pancreatic tumor cells, because of their high expression levels of NRG (26). Accordingly, when singly applied, our NRG-competitive NG33 Ab better than the other mAbs, inhibited BXPC3 tumors (Fig. 6). Importantly, NG33 not only displaced NRG better than the other mAbs; it also induced stronger ADCC and more extensive degradation of HER3. Because other Abs induced some degradation and only weakly elevated ADCC, but their antitumor activities were quite limited, we tend to attribute the superiority of NG33 to the blockade of autocrine loops involving HER3 and the many NRG isoforms it can bind. It is worthwhile mentioning that the NRGs are highly expressed in carcinomas (34). Moreover, the mechanism of action of cetuximab, an anti-EGFR Ab used to treat colorectal cancer, has been attributed to blockade of EGFR-specific ligands like amphiregulin (35). Likewise, ovarian tumors might depend on an autocrine loop involving HER3 and NRG1 (36).

In an effort to enhance the antitumor action of our most potent Ab, NG33, we combined it with a second Ab, for example, NG83 or NG140, which resulted in relatively small improvements of the inhibitory effect. This result is rather surprising, considering the clearly additive or synergistic effects induced by mAb combinations targeting EGFR (19) or HER2 (20, 21). Considering the relatively weak difference between mAbs used alone and mAb combinations at inducing HER3 degradation, one might speculate that the frequent overexpression of EGFR and HER2, but rare overexpression of HER3, underlays the weak additive effects observed when combining anti-HER3 mAbs. One important example, an Ab combination targeting EGFR, called Sym004, is currently being tested in clinical trials that recruited colorectal cancer (37) and non-small-cell lung cancer (38) patients. Interestingly, although one of our mAbs, XC252, accelerated HER3 degradation and decreased BXPC3 proliferation in vitro, this mAb did not enhance the ability of NG33 to inhibit BXPC3

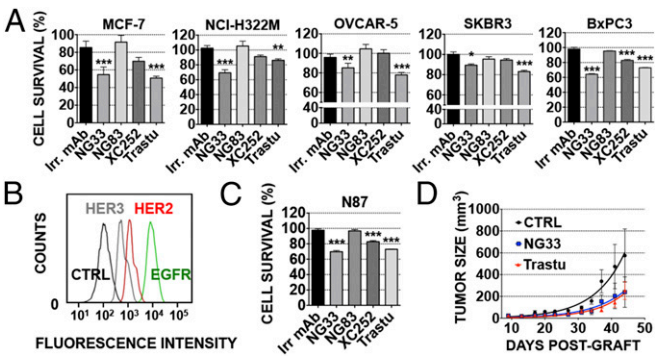

Fig. 4. Anti-HER3 mAbs decrease NRG-induced tumor cell survival, both in vitro and in animals, as effectively as trastuzumab. (*A* and *C*) Proliferation assays using MTT were performed on five different cell lines, as indicated. Cells (5,000 per well) were plated the day before and treated for 72 h with the various agents (each at 10 μg/mL) in medium supplemented with NRG (10 ng/mL). Trastuzumab (*Trastu*) indicates a huminazed mAb to HER2/ERBB2. (*B*) N87 cells were incubated for 1 h at 4 °C with mAbs (each at 10 μg/mL) directed to EGFR (565), HER2 (L26), or HER3 (XC252). After two washes, the cells were incubated for 1 h at 4 °C (in the dark) with a secondary anti-mouse Ab coupled to Alexa Fluor 488. Fluorescence intensity (F.I.) was measured by using the LSRII flow cytometer. N87 cell survival was determined as in *A*. (*D*) CD1-nude mice were grafted s.c. with 5×10^6 N87 cells. Once tumors became palpable (after ~13 d), the mice were randomized into group of six animals and treated twice a week for 5 wk. The control group (CTRL) was injected intraperitoneally (IP) with saline (200 μL). The other groups were treated with mAbs at the final concentration of 0.2 mg/0.2 mL of saline per mouse. The mice were weighed once a week, and the tumors were measured twice a week. The average tumor size measured in six mice (± SEM) is shown. ***$P < 0.001$; **$P < 0.01$ (ANOVA and post hoc tests).

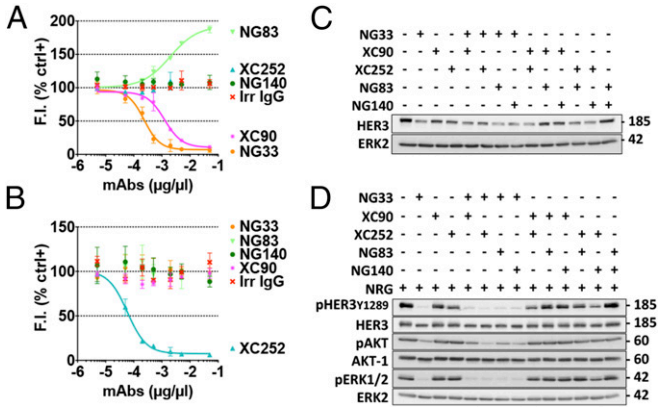

Fig. 5. Pairwise applications of Abs directed at distinct epitopes of HER3. (*A* and *B*) The Abs NG33 and XC252 were labeled with the fluorescent dye Lumi4 Tb Cryptate (K2). The 96-well plates were coated with IgB3 (1.5 μg/mL) and incubated for 1 h with various concentrations of mAbs. The labeled mAb, NG33-K2 (*A*) or XC252-K2 (*B*), was then added at 1 nM final concentration. Fluorescence intensity (at 610 nm) was measured after an hour-long incubation. (*C*) The indicated combinations of anti-HER3 mAbs were studied for their ability to trigger HER3 degradation using N87 cells. Cells were treated for 2 h at 37 °C with mAbs (10 μg/mL). Protein samples were subjected to immunoblotting by using the indicated Abs. (*D*) The combination's capacity to modulate NRG-induced phosphorylation of HER3, AKT, and ERK was evaluated by using N87 cells. After 20 min of treatment at 37 °C with the indicated mAbs (10 μg/mL), NRG (20 ng/mL) was added to the cells and incubated for 10 min. Thereafter, the cells were lysed, and equal quantities of lysate proteins were electrophoresed before immunoblotting, as indicated.

tumors. Lack of added benefit might be attributed to the relatively weak ability of XC252 to trigger ADCC in vitro. Notably, a study that combined three mAbs to HER2 concluded that enhanced ADCC might explain synergistic mAb effects on tumor growth (39).

We previously proposed that a "surface lattice" formed by transmembrane receptors cross-linked by two or more Abs might underlay the enhanced ability of certain mAb combinations to accelerate receptor degradation in vitro and inhibit tumor growth in animals (18, 20, 21). According to this model, the aggregated receptors are recognized by the endocytosis machinery and are subsequently sorted for degradation in lysosomes in a dynamin-dependent manner (19). Cross-linked HER3 molecules might deviate from the lattice model. For one, HER3 harbors a defective kinase domain (8), and it is uncoupled from GRB2, an adaptor needed for robust endocytosis of EGFR (40, 41). Endocytosis and degradation of EGFR family members are controlled by their kinase activity, which recruits the CBL ubiquitin ligase (42). By contrast, HER3 needs no ligand or autophosphorylation to undergo endocytosis (43), which is frequently followed by rapid recycling back to the plasma membrane (44). Moreover, HER3 down-regulation involves both a deubiquitinating enzyme, USP8, and a ubiquitin ligase, Nrdp1 (45). HER3 also interacts with NEDD4, a HECT family E3 ubiquitin ligase (46). These differences, along with the relatively low expression levels of HER3, might explain the lack of benefit of combining two anti-HER3 Abs.

In summary, our set of anti-HER3 Abs reduces the attractiveness of the option of combining two or more Abs to improve the antitumor effects of Abs to NRG receptors. Independently, our studies strengthen the possibility attributing to NRGs and their low affinity receptor, HER3, a driving role in tumor progression. This role is analogous to the mechanism underlying the therapeutic effect of anti-EGFRs such as panitumumab in colorectal cancer (35, 47). Future studies should address the intriguing possibility that different types of carcinoma depend on distinct members of the EGF/NRG family for their tumorigenic growth and also for evasion of the cytotoxic effects of chemotherapy.

Materials and Methods

Generation of mAbs to HER3. Mice immunization, fusion between myeloma cells and splenocytes, and the subsequent hybridoma subcloning were performed as described (24). Hybridoma supernatant screening, using ELISA, was performed on 96 well-plates coated with IgB3 (1 μg/mL) or with a human IgG molecule (1 μg/mL). The plates were blocked with PBS containing BSA (1%; weight/vol) and incubated for 1 h with hybridoma supernatants, followed by a second incubation (60 min) with HRP-labeled anti-mouse IgG and subsequent detection using 2,2′-azino-bis(3-ethylbenzothiazoline-6-sulfonic acid). The second step of the screening was performed by immunoprecipitation. Anti-mouse IgG agarose beads were incubated first with 100 μL of hybridoma supernatant and subsequently with whole-cell lysate from HER3-expressing T47D cells. The mAbs directed to HER3 were then isotyped by using the SBA Clonotyping System/HRP kit (SouthernBiotech).

Tag-lite HER3 Binding Assay. A Tag-lite plasmid coding for HER3 fused to SNAP-tag (CISbio bioassays) was transiently expressed in HEK-293 cells. Cells were plated and labeled 24 h after transfection with 200 nM SNAP-Lumi4-Tb substrate (donated by CISbio bioassays) in Tag-lite labeling medium (1 h at 37 °C). Abs (100 μL at 1–2 mg/mL) were labeled with the d2 dye (acceptor). A set of 16 twofold serial dilutions spanning from 0.006 nM to 200 nM of labeled Ab (Ab-d2) were prepared in Tag-lite labeling medium. The specific signal was obtained by mixing cells (10,000 cells in 10 μL per well), 5 μL of Ab-d2 from the serial dilution and 5 μL of Tag-lite labeling medium. The nonspecific signal was obtained by mixing 10 μL of cells with 5 μL of the corresponding unlabeled Ab (300 nM) and 5 μL of Ab-d2 conjugate from the serial dilution. After overnight incubation at 20 °C, time-resolved (TR) fluorescence

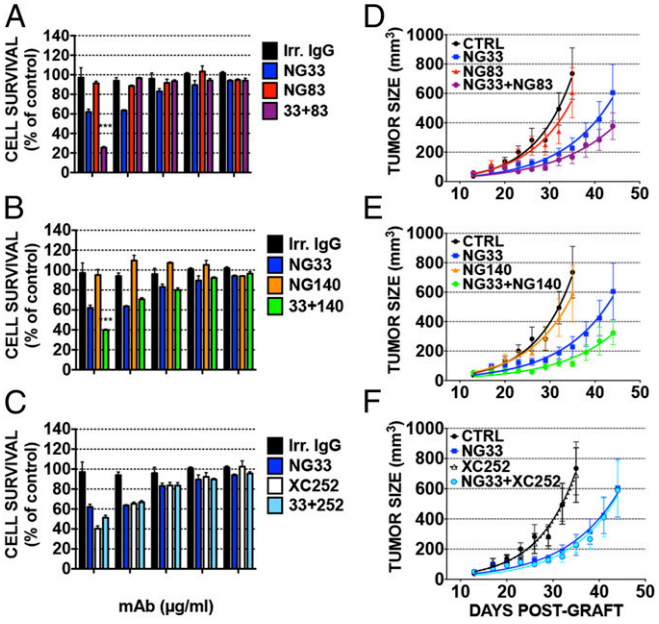

Fig. 6. Both in vitro and in animals, combinations of noncompetitive mAbs to HER3 only weakly enhance the inhibitory effects of the respective single Abs. (*A–C*) Proliferation assays using MTT were performed on BXPC3 cells (5,000 cells per well). Cells were plated on the day before and treated for 72 h with the indicated mAbs. Increasing concentrations of the indicated mAbs (either alone or in combination) were used in medium supplemented with 1% serum and NRG (10 ng/mL). An irrelevant IgG fraction was used as control. (*D–F*) CD1-nude mice were grafted s.c. with 5×10^6 BXPC3 cells. Once tumors became palpable (after 13 d), the mice were randomized into groups of eight animals and treated once every 3 d for 5 wk. The control group (CTRL) was injected intraperitoneally (IP) with 200 μL of PBS. The other groups were treated with the indicated mAbs, either alone or in combinations, at a final concentration of 0.2 mg/0.2 mL saline per mouse. Body weight was determined once a week, and the tumors were measured twice a week. Shown are average tumor sizes from seven or eight mice (±SEM).

was measured on a Pherastar FS reader. The E665/E620 ratio was computed, and values, measuring TR-FRET, were plotted against Ab concentration.

ADCC Assays. ADCC was evaluated by using a luciferase assay. BXPC3-luc cells (4,000 per well) were preincubated in microplates for 30 min with the Abs. Thereafter, Ficoll-purified human peripheral blood mononuclear cells from buffy coats were added at a 10:1 effector to target cell ratio (E:T). After 24 h at 37 °C, the supernatant was removed, and luciferine (Promega) was added. Bioluminescence was determined by using the Wallac Trilux 1450 Microbeta liquid scintillation and luminescence counter (Perkin-Elmer). The percentage of cellular cytotoxicity was calculated by using the following formula: percentage of specific lysis = [bioluminescence in experimental point − basal bioluminescence]/[bioluminescence in total lysis − basal bioluminescence] × 100. Basal bioluminescence was obtained when BXPC3-Luc cells were incubated with hPBMC alone. Likewise, bioluminescence in total lysates was obtained after a 30-min incubation of BXPC3-Luc in the presence of SDS (0.1%).

Tumorigenic Growth in Mice. All animal studies were approved by the Weizmann Institute's Review Board. Tumor bearing CD1-nude mice were randomized into groups of eight mice and injected s.c. in the right flank with cancer cells (5×10^6 per mouse). mAbs were injected intraperitoneally at 200 μg per mouse per injection, twice a week, for 5 wk. Tumor volume and body weight were evaluated twice and once per week, respectively. Mice were euthanized when tumor size reached 1,500 mm^3.

ACKNOWLEDGMENTS. We thank Bilha Schechter and Ruth Maron for their insightful advice regarding the in vivo experiments; Yaniv Levi for taking care of the animals; and both Hedva Hamawi and Ziv Landau for their assistance in the hybridoma generation process. Our laboratories are supported by the Israel Cancer Research Fund, the M. D. Moross Cancer Research Institute, and the Dr. Miriam and Sheldon G. Adelson Medical Research Foundation. Y.Y. is the incumbent of the Harold and Zelda Goldenberg Professorial Chair. M.S. is the incumbent of the W. Garfield Weston Chair.

1. Witsch E, Sela M, Yarden Y (2010) Roles for growth factors in cancer progression. *Physiology (Bethesda)* 25(2):85–101.
2. Barros FF, Powe DG, Ellis IO, Green AR (2010) Understanding the HER family in breast cancer: Interaction with ligands, dimerization and treatments. *Histopathology* 56(5): 560–572.
3. Lax I, et al. (1988) Localization of a major receptor-binding domain for epidermal growth factor by affinity labeling. *Mol Cell Biol* 8(4):1831–1834.
4. Burgess AW (2008) EGFR family: Structure physiology signalling and therapeutic targets. *Growth Factors* 26(5):263–274.
5. Clayton AH, et al. (2005) Ligand-induced dimer-tetramer transition during the activation of the cell surface epidermal growth factor receptor—A multidimensional microscopy analysis. *J Biol Chem* 280(34):30392–30399.
6. Garrett TP, et al. (2002) Crystal structure of a truncated epidermal growth factor receptor extracellular domain bound to transforming growth factor alpha. *Cell* 110(6): 763–773.
7. Yarden Y, Sliwkowski MX (2001) Untangling the ErbB signalling network. *Nat Rev Mol Cell Biol* 2(2):127–137.
8. Shi F, Telesco SE, Liu Y, Radhakrishnan R, Lemmon MA (2010) ErbB3/HER3 intracellular domain is competent to bind ATP and catalyze autophosphorylation. *Proc Natl Acad Sci USA* 107(17):7692–7697.
9. Jaiswal BS, et al. (2013) Oncogenic ERBB3 mutations in human cancers. *Cancer Cell* 23(5):603–617.
10. Lurje G, Lenz HJ (2009) EGFR signaling and drug discovery. *Oncology* 77(6):400–410.
11. Schmitz KR, Ferguson KM (2009) Interaction of antibodies with ErbB receptor extracellular regions. *Exp Cell Res* 315(4):659–670.
12. Narayan M, et al. (2009) Trastuzumab-induced HER reprogramming in "resistant" breast carcinoma cells. *Cancer Res* 69(6):2191–2194.
13. Garrett JT, et al. (2011) Transcriptional and posttranslational up-regulation of HER3 (ErbB3) compensates for inhibition of the HER2 tyrosine kinase. *Proc Natl Acad Sci USA* 108(12):5021–5026.
14. Lu Y, et al. (2007) Epidermal growth factor receptor (EGFR) ubiquitination as a mechanism of acquired resistance escaping treatment by the anti-EGFR monoclonal antibody cetuximab. *Cancer Res* 67(17):8240–8247.
15. Wheeler DL, et al. (2008) Mechanisms of acquired resistance to cetuximab: Role of HER (ErbB) family members. *Oncogene* 27(28):3944–3956.
16. Desbois-Mouthon C, et al. (2009) Insulin-like growth factor-1 receptor inhibition induces a resistance mechanism via the epidermal growth factor receptor/HER3/AKT signaling pathway: Rational basis for cotargeting insulin-like growth factor-1 receptor and epidermal growth factor receptor in hepatocellular carcinoma. *Clin Cancer Res* 15(17):5445–5456.
17. Kruser TJ, Wheeler DL (2010) Mechanisms of resistance to HER family targeting antibodies. *Exp Cell Res* 316(7):1083–1100.
18. Ben-Kasus T, Schechter B, Sela M, Yarden Y (2007) Cancer therapeutic antibodies come of age: Targeting minimal residual disease. *Mol Oncol* 1(1):42–54.
19. Ferraro DA, et al. (2013) Inhibition of triple-negative breast cancer models by combinations of antibodies to EGFR. *Proc Natl Acad Sci USA* 110(5):1815–1820.
20. Ben-Kasus T, Schechter B, Lavi S, Yarden Y, Sela M (2009) Persistent elimination of ErbB-2/HER2-overexpressing tumors using combinations of monoclonal antibodies: Relevance of receptor endocytosis. *Proc Natl Acad Sci USA* 106(9):3294–3299.
21. Friedman LM, et al. (2005) Synergistic down-regulation of receptor tyrosine kinases by combinations of mAbs: Implications for cancer immunotherapy. *Proc Natl Acad Sci USA* 102(6):1915–1920.
22. Miles D, et al. (2013) Treatment of older patients with HER2-positive metastatic breast cancer with pertuzumab, trastuzumab, and docetaxel: Subgroup analyses from a randomized, double-blind, placebo-controlled phase III trial (CLEOPATRA). *Breast Cancer Res Treat* 142(1):89–99.
23. Gala K, Chandarlapaty S (2014) Molecular pathways: HER3 targeted therapy. *Clin Cancer Res* 20(6):1410–1416.
24. Chen X, et al. (1996) An immunological approach reveals biological differences between the two NDF/heregulin receptors, ErbB-3 and ErbB-4. *J Biol Chem* 271(13): 7620–7629.
25. Lazrek Y, et al. (2013) Anti-HER3 domain 1 and 3 antibodies reduce tumor growth by hindering HER2/HER3 dimerization and AKT-induced MDM2, XIAP, and FoxO1 phosphorylation. *Neoplasia* 15(3):335–347.
26. Thomas G, et al. (2014) HER3 as biomarker and therapeutic target in pancreatic cancer: New insights in pertuzumab therapy in preclinical models. *Oncotarget* 5(16): 7138–7148.
27. Aurisicchio L, Marra E, Roscilli G, Mancini R, Ciliberto G (2012) The promise of anti-ErbB3 monoclonals as new cancer therapeutics. *Oncotarget* 3(8):744–758.
28. Baselga J, Swain SM (2009) Novel anticancer targets: Revisiting ERBB2 and discovering ERBB3. *Nat Rev Cancer* 9(7):463–475.
29. Jiang N, Saba NF, Chen ZG (2012) Advances in targeting HER3 as an anticancer therapy. *Chemother Res Pract* 2012:817304.
30. Kol A, et al. (2014) HER3, serious partner in crime: Therapeutic approaches and potential biomarkers for effect of HER3-targeting. *Pharmacol Ther* 143(1):1–11.
31. Pedersen MW, et al. (2010) Sym004: A novel synergistic anti-epidermal growth factor receptor antibody mixture with superior anticancer efficacy. *Cancer Res* 70(2):588–597.
32. Drebin JA, Link VC, Greene MI (1988) Monoclonal antibodies reactive with distinct domains of the neu oncogene-encoded p185 molecule exert synergistic anti-tumor effects in vivo. *Oncogene* 2(3):273–277.
33. Kasprzyk PG, Song SU, Di Fiore PP, King CR (1992) Therapy of an animal model of human gastric cancer using a combination of anti-erbB-2 monoclonal antibodies. *Cancer Res* 52(10):2771–2776.
34. Révillion F, Lhotellier V, Hornez L, Bonneterre J, Peyrat JP (2008) ErbB/HER ligands in human breast cancer, and relationships with their receptors, the bio-pathological features and prognosis. *Ann Oncol* 19(1):73–80.
35. Khambata-Ford S, et al. (2007) Expression of epiregulin and amphiregulin and K-ras mutation status predict disease control in metastatic colorectal cancer patients treated with cetuximab. *J Clin Oncol* 25(22):3230–3237.
36. Sheng Q, et al. (2010) An activated ErbB3/NRG1 autocrine loop supports in vivo proliferation in ovarian cancer cells. *Cancer Cell* 17(3):298–310.
37. Dienstmann R, et al. (2013) Proof-of-concept study of Sym004, an anti-EGFR monoclonal antibody (mAb) mixture, in patients (pts) with anti-EGFR mab-refractory KRAS wild-type (wt) metastatic colorectal cancer (mCRC). *J Clin Oncol* 31(15 Suppl):abstr 3551.
38. Machiels J-PH, et al. (2013) Sym004, a novel strategy to target EGFR with an antibody mixture, in patients with advanced SCCHN progressing after anti-EGFR monoclonal antibody: A proof of concept study. *J Clin Oncol* 31(15 Suppl):abstr 6002.
39. Spiridon CI, et al. (2002) Targeting multiple Her-2 epitopes with monoclonal antibodies results in improved antigrowth activity of a human breast cancer cell line in vitro and in vivo. *Clin Cancer Res* 8(6):1720–1730.
40. Waterman H, et al. (2002) A mutant EGF-receptor defective in ubiquitylation and endocytosis unveils a role for Grb2 in negative signaling. *EMBO J* 21(3):303–313.
41. Jiang X, Huang F, Marusyk A, Sorkin A (2003) Grb2 regulates internalization of EGF receptors through clathrin-coated pits. *Mol Biol Cell* 14(3):858–870.
42. Levkowitz G, et al. (1999) Ubiquitin ligase activity and tyrosine phosphorylation underlie suppression of growth factor signaling by c-Cbl/Sli-1. *Mol Cell* 4(6):1029–1040.
43. Sak MM, et al. (2012) The oncoprotein ErbB3 is endocytosed in the absence of added ligand in a clathrin-dependent manner. *Carcinogenesis* 33(5):1031–1039.
44. Waterman H, Sabanai I, Geiger B, Yarden Y (1998) Alternative intracellular routing of ErbB receptors may determine signaling potency. *J Biol Chem* 273(22):13819–13827.
45. Cao Z, Wu X, Yen L, Sweeney C, Carraway KL, 3rd (2007) Neuregulin-induced ErbB3 downregulation is mediated by a protein stability cascade involving the E3 ubiquitin ligase Nrdp1. *Mol Cell Biol* 27(6):2180–2188.
46. Huang Z, et al. (2014) The E3 ubiquitin ligase NEDD4 negatively regulates HER3/ErbB3 level and signaling. *Oncogene*.
47. Jacobs B, et al. (2009) Amphiregulin and epiregulin mRNA expression in primary tumors predicts outcome in metastatic colorectal cancer treated with cetuximab. *J Clin Oncol* 27(30):5068–5074.